IX International Conference on Computational Methods in Marine Engineering
MARINE 2021
I.M. Viola and F. Brennan (Eds)

URANS SIMULATIONS OF THE JAPANESE BULK CARRIER BENCHMARK TEST CASE

August C. Sturm* **and Kevin J. Maki***,†

*Department of Naval Architecture and Marine Engineering
University of Michigan
Ann Arbor, MI USA 48109-2145
†e-mail: kjmaki@umich.edu

Key words: Calm-water resistance, stern-flow, RANS, validation

Abstract. This paper presents computations for the flow around the Japanese Bulk Carrier (JBC) international benchmark case operating in calm-water. The flow is computed with the OpenFOAM opensource software. The purpose to perform the computations is to participate in an open validation study where the grids and results are provided together with the paper in a special session. Results of the wave elevation, force on the hull, and velocity in the stern region are provided on a series of seven computational grids.

1 INTRODUCTION

Computational fluid dynamics for calm-water resistance and flow field prediction has been under steady development for decades, yet challenges still remain in selecting the proper grid layout, turbulence model, near-wall model, and flow-solution strategy. Computational technology is driven with contributions from academia, industrial users, governmental agencies, and software companies. An important step in the development of new methods is the participation in international benchmark studies [5, 3].

For the MARINE 2021 Conference a special session is organized to compute the flow around the JBC in calm water with the goal of making the computations available after the workshop. In this paper the flow is computed using OpenFOAM version 18.06.

1.1 Japanese Bulk Carrier Test Case

One of the test cases in the 2015 Tokyo Workshop [3] was the Japanese Bulk Carrier (JBC). This hull is used to assess how different numerical codes can predict the effects of an energy saving device (ESD). Participants use different turbulence models, flow solvers, grid densities, and results are compared with different experimental measurements at model scale. This hull form is characterized by a service speed of 14.5 to 15.5 kn, corresponding to Froude number of approximately 0.15, and block coefficient of 0.82 to 0.85 (depending on draft). The relatively low Froude number means that free-surface waves play a small role in the total resistance prediction,

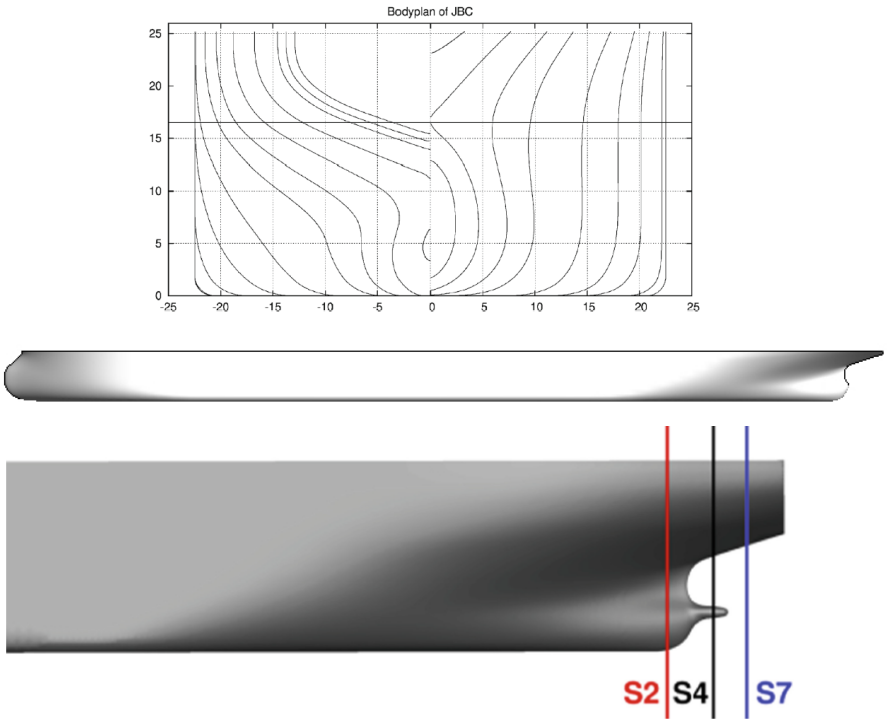

Figure 1: Lines and side view of JBC hull.

and the relatively high block coefficient means that viscous flow and possible separation will play a large role in the flow into the propeller. Energy saving devices can typically save several percent or more of the required power. This means that the numerical uncertainty should ideally be smaller than this, and the flow into the propeller must be accurate. The body plan and side view of the hull are shown in Figure 1.

2 FLOW SOLVER AND COMPUTATIONAL GRIDS

The flow is computed with a custom solver built with the OpenFOAM opensource toolkit, version 18.06. The starting point of the solver is the `interDyMFoam` solver. The flow solver is customized by using a specific motion solver that brings the body from rest to the final forward speed. The body accelerates over a user defined time interval (in the same way that a physical model is accelerated from rest in a towing tank)[1, 9], while the sinkage and trim is solved with a stable and time-accurate equation of motion solver[7]. The reason that the equations are written in an earth fixed coordinate is because if the body is started impulsively from rest, there would be a significant wave field that is generated due to the impulsive start, and it takes a long time for the transient waves to be damped by viscosity or with damping zones or boundary conditions. This is a well known phenomenon and an analytical description can be found in [6],[8, pg 617]. A second customization is the manner in which waves are generated or damped. The `waves2Foam`[4] library is used with implicit under-relaxation of the flow velocity and volume-of-fluid field to enforce calm-water conditions at the domain extents.

The computational grids are generated with the `snappyHexMesh` tool that is provided with OpenFOAM. Grids of different resolution on the body, free-surface, and stern region are generated by varying the refinement of the starting background grid, or the refinement level within the `snappyHexMesh` generation stage. The grids represent an evolution from the first test grid to those with improved layout and resolution. It is important to note that grids G2 and G3 are identical with the exception that G3 has a refinement block around the free-surface. The same is true for grids G5 and G6. Note that adding the refinement block adds up to 12% additional cell count, but doubles the resolution of the wave field. The grids have near wall spacing corresponding to $7 < y^+_{\text{avg}} < 32$.

An important validation quantity for this hull is the velocity field in the stern region. The flow field is measured and computed in three transverse planes, labeled S2, S4, and S7 (see Figure 1). The grid resolution for these three planes is shown in Figure 2.

Table 1: Mesh Study Statistics

	G1	G2	G3	G4	G5	G6	G7
# cells (million)	3.03	3.07	3.36	8.48	16.2	18.2	18.9
b.l. coverage (%)	99.3	94.8	95.4	99.5	99.2	99.7	99.2
y^+ (average)	24	32	32	15	23	7	23
near-wall spacing (mm)	1.41	1.89	1.89	0.94	1.41	0.47	1.41
run time (hr)	14.98	19.9	16.37	67.88	55.27	115.20	65.41
number of cores	32	36	36	36	72	72	72

2.1 Flow Conditions

The flow conditions are set according to to cases 1.1a and 1.3a of the 2015 Tokyo Workshop [3]. Table 2 contains a summary of the flow conditions. The water model is towed free to sink and trim in calm water. To compare with the experimental data there is no propeller, rudder, nor ESD.

3 RESULTS

3.1 Forces and Motion

The model is accelerated to the final speed over a time period of six seconds. The total force for each of the seven grids is shown in Figure 3. In this figure the experimental measurement and the average from 19 submissions in Tokyo 2015 are plotted. Note the total force takes a maximum around 4 s, and then quickly drops an oscillates around the final mean value. The oscillation is related to the flow domain width and depth, the gravity and forward speed, and the location of the damping zone applied with `waves2Foam`. Also the amplitude of the oscillation is determined by magnitude of the acceleration used to reach the final speed. If a shorter time period were used, the overshoot and resulting amplitude of oscillation would be larger. Also shown in Figure 3 are the time histories of the frictional force, together with the average of the

Table 2: Case Parameters

Parameter	Value	Unit
scale factor	40	-
L_{pp}	7	m
U	1.179	m/s
g	9.8	m/s^2
R_e	7.46×10^6	-
ρ_{water}	998.2	kg/m^3
ρ_{air}	1.5	kg/m^3
ν_{water}	1.11×10^{-6}	m^2/s
ν_{air}	1.50×10^{-5}	m^2/s
S_o	12.2206	m^2

frictional force from the Tokyo 2015 workshop.

The mean value and standard deviation is computed over the last 15 s of each time record. The mean force coefficients are shown in Figure 4. Note that in this figure the error bar on the Tokyo 2015 participants represents the standard deviation of 19 submissions, whereas the error bars on the current results represents the standard deviation from the oscillation in time. While the oscillations in time may appear small in Figure 3, it is not insignificant when comparing to the experimental value or the average of the Tokyo 2015 submissions. Also, the variation in time is almost entirely due to the oscillation in the pressure force due to the slowly moving waves in the domain.

The coarsest G1 shows a slight over-prediction of force compared to G2-7, the average of the T2015 submissions, and the experiment. The variation in the frictional force for different values of near-wall spacing is very small, which indicates the adaptive wall function is working in a practical manner for the the purpose of frictional drag prediction.

The sinkage and trim time histories are shown in Figure 5. Also in this figure the experimental value, and the mean of the numerical predictions to the Tokyo 2015 workshop are shown. The shaded area shows one standard deviation amongst the 14 submissions to T2015. The present results show very small difference among the seven grids for both sinkage and trim. The comparison with experiment and other numerical results also show very good agreement, although the present results show a slightly larger bow-down trim.

3.2 Wave Profiles

Figure 6 shows the wave profile on the hull, and at two lateral slices of $y/L = 0.1403$ and 0.19. Also shown are the experimental measurements. Note that at this Froude number the waves are short relative to the ship length. The longest transverse wave λ_T can be approximated as

$$\frac{\lambda_T}{L_{\text{pp}}} = 2\pi F^2,$$

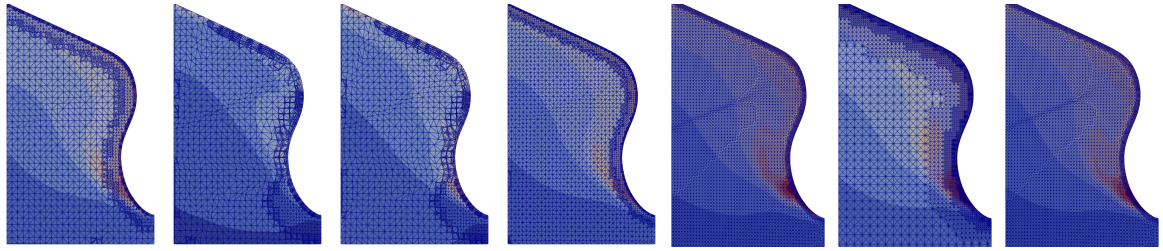

(a) S2, G1-7 from left to right

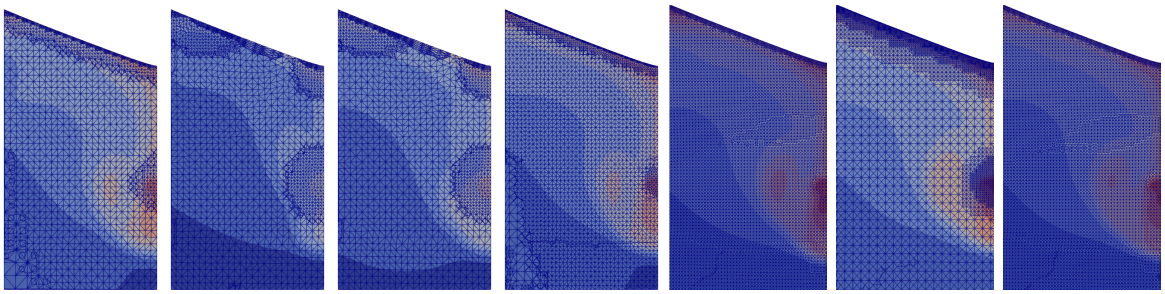

(b) S4, G1-7 from left to right

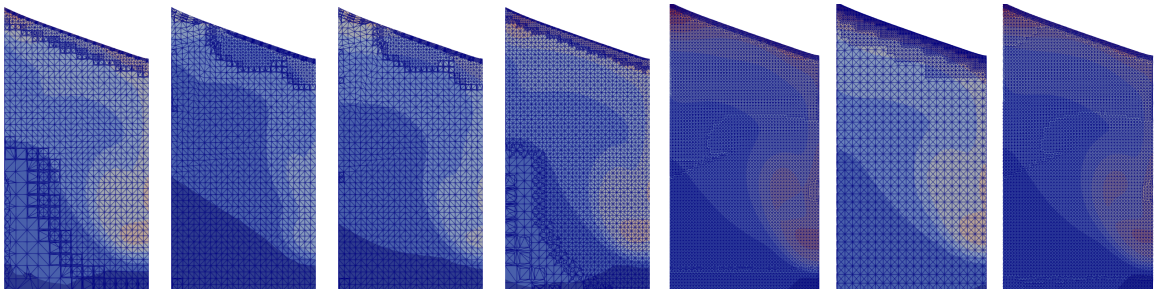

(c) S7, G1-7 from left to right

Figure 2: Comparison of grid resolution in stern planes S2, S4, and S7

which in this case yields approximately 7 waves per ship length. This can be seen in each of the wave cuts.

The results for G1 show significant difference with the other grids and the experiments. Also for the furthest wave cut G2 shows significant discretization error. Whereas G3, which is the same as G2 but with a refinement block around the free-surface plane, shows an improved comparison with the experiments.

3.3 Flow Field in Stern Region

The flow into the propeller region is fundamental for the assessment of an ESD. In this work the Spalart-Allmaras turbulence model is used, and this model has the propensity to underpredict separation. The numerical results are shown for the three planes labeled S2, S4, and S7 (see Figure 1). Experimental data are available for S2.

Figure 7 shows the numerical results for the axial velocity at planes S2, S4, and S7, on each of

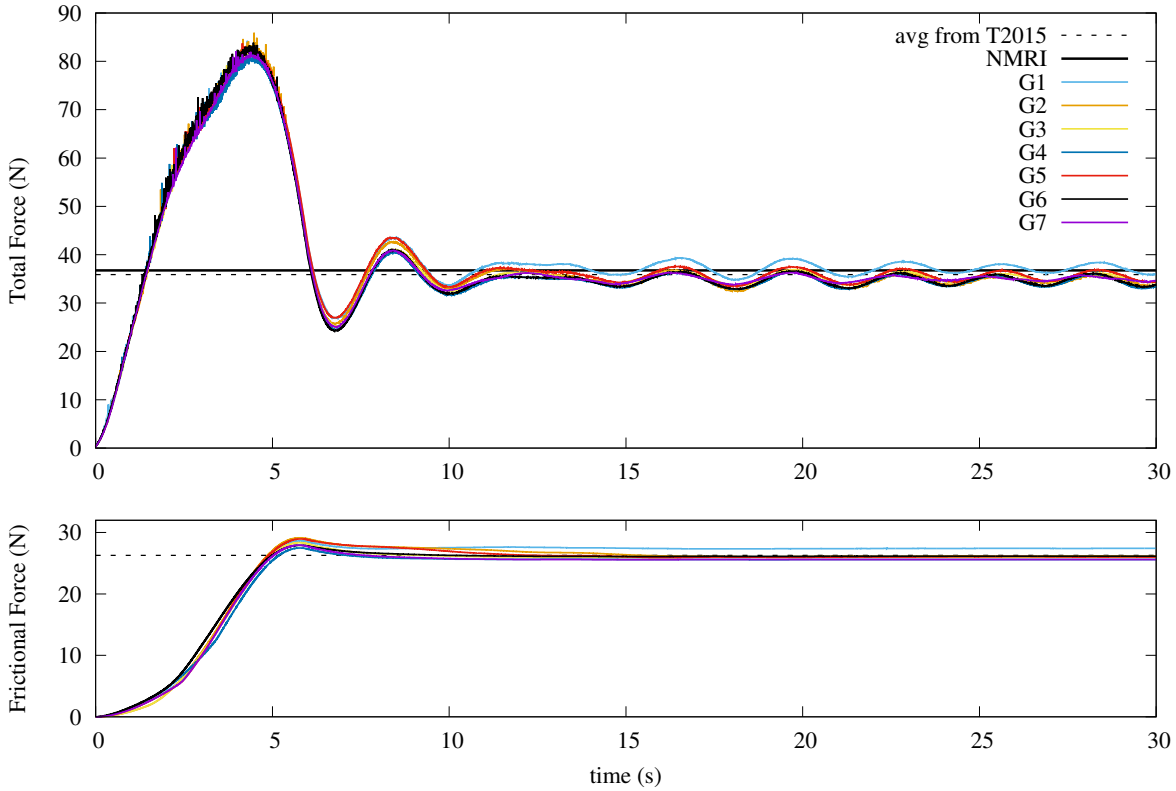

Figure 3: Total Force (*top*) and frictional force (*bottom*) time history.

the seven grids. For plane S2, the experimental data show a region of low velocity corresponding to a vortex core that appears near the hourglass part of this station. None of the seven numerical grids exhibit the full vortex core as seen in the experiment, although the finer grids, G5–G7 show the remnants of such a flow structure.

Stations S4 and S7 show a similar pattern. The refined grids G5–G7 show a more distinct formation of the low velocity region associated with the strong vortex core that travels through the propeller plane region.

4 CONCLUSIONS

In this paper CFD computations are performed for the JBC international benchmark case for calm-water operation. A series of seven grids are used that represent the evolution of grids that are generated while learning how to perform computations of this hull form. The flow is computed with the OpenFOAM opensource CFD software version 18.06. The results are to be made available as part of the special session on structured validation of CFD codes for ship hydrodynamics prediction.

Quantities of forces and motion show that all seven grids are able to predict the drag, sinkage and trim with good accuracy. Only the first grid that was used shows a slight overprediction of drag. Also, the near-wall grids range from $7 < y^+_{\text{avg}} < 32$, and the frictional force varies by less

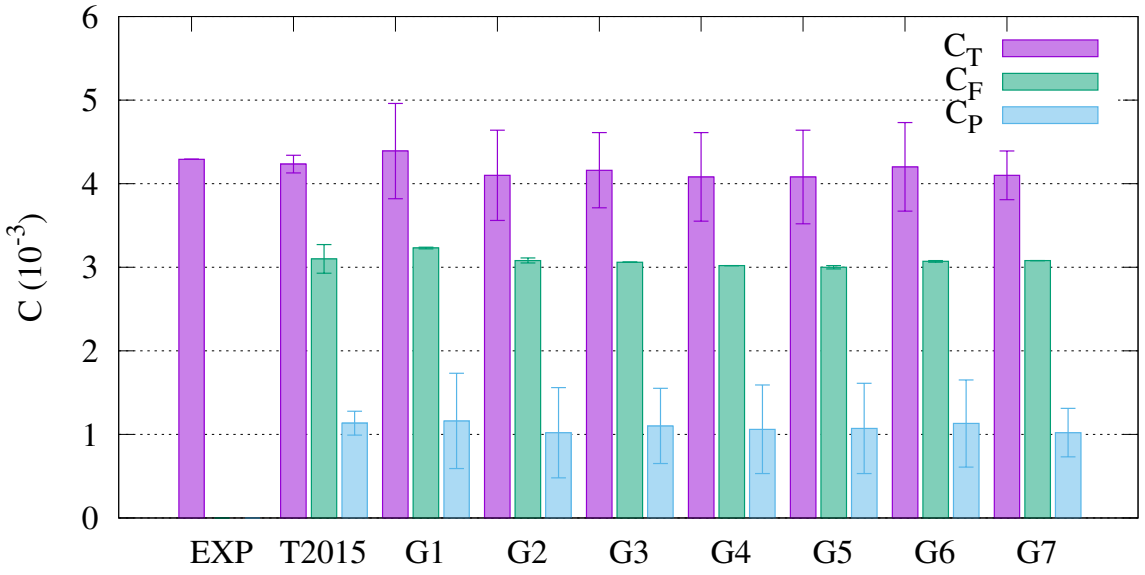

Figure 4: Force coefficient comparison. Errorbars on T2015 submissions represent standard deviation among participants, errorbars on present data represent standard deviation of time history averaged over time window 15 to 30 s.

than 2% over this range of near-wall spacing. This indicates that the adaptive wall-function is working well from a practical standpoint.

The free-surface profiles are in close agreement with the experiment. It is shown that a relatively coarse grid with local refinement is able to resolve the wave field with good accuracy.

The flow field in the propeller plane shows attached flow, where as the experiment shows a strong vortex core that is only partially visible in the CFD results.

REFERENCES

[1] G. P. Filip, W. Xu, and K. J. Maki. Urans predictions of resistance and motions of the kcs in head waves. Technical report, University of Michigan, 2017.

[2] Nobuyuki Hirata, Hiroshi Kobayashi, Takanori Hino, Yasuyuki Toda, Moustafa Abdel-Maksoud, and Frederick Stern Experimental Data for JBC Resistance, Sinkage, Trim, Self-Propulsion Factors, Longitudina lWave Cut and Detailed Flow with and without an Energy Saving Circular Duct. Technical report, National Maritime Research Institute, Mitaka, Japan, 2015.

[3] T. Hino, F. Stern, L. Larsson, M. Visonneau, N. Hirata, and J. Kim. *Numerical Ship Hydrodynamics: An Assessment of the Tokyo 2015 Workshop*, volume 94. Springer Nature, 2017.

[4] N. G. Jacobsen, D. R. Fuhrman, and J. Fredsoe. A wave generation toolbox for the open-source cfd library: Openfoam. *Int. J. Numer. Meth. Fluids*, 70(9):1073–1088, 2012.

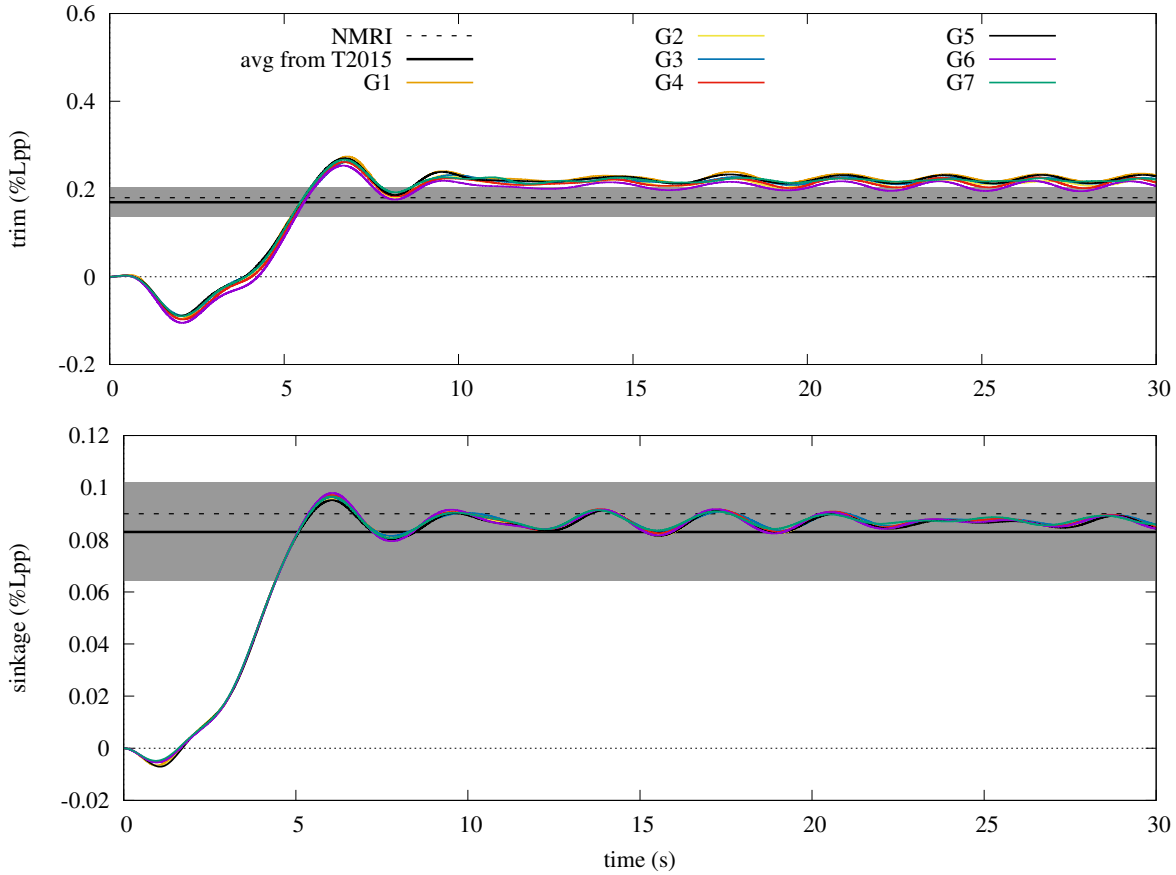

Figure 5: Trim (*top*) and sinkage (*bottom*) time history.

[5] L. Larsson, F. Stern, and M. Visonneau. *Numerical ship hydrodynamics: an assessment of the Gothenburg 2010 workshop*. Springer, 2013.

[6] F. Ursell. The decay of the free motion of a floating body. *J. Fluid Mech.*, 19:305–319, 1964.

[7] D. Piro and K. Maki. Hydroelastic analysis of bodies that enter and exit water. *Journal of Fluids and Structures*, 37:134–150, 2013.

[8] J. Wehausen and E. Laitone. *Surface Waves*, volume 9 of *Encyclopedia of Physics: Fluid Dynamics III*. Springer-Verlag, Berlin, 1960.

[9] W. Xu, G. Filip, and K. J. Maki. A method for the prediction of extreme ship responses using design-event theory and computational fluid dynamics. *Journal of Ship Research*, 64(1), 2020.

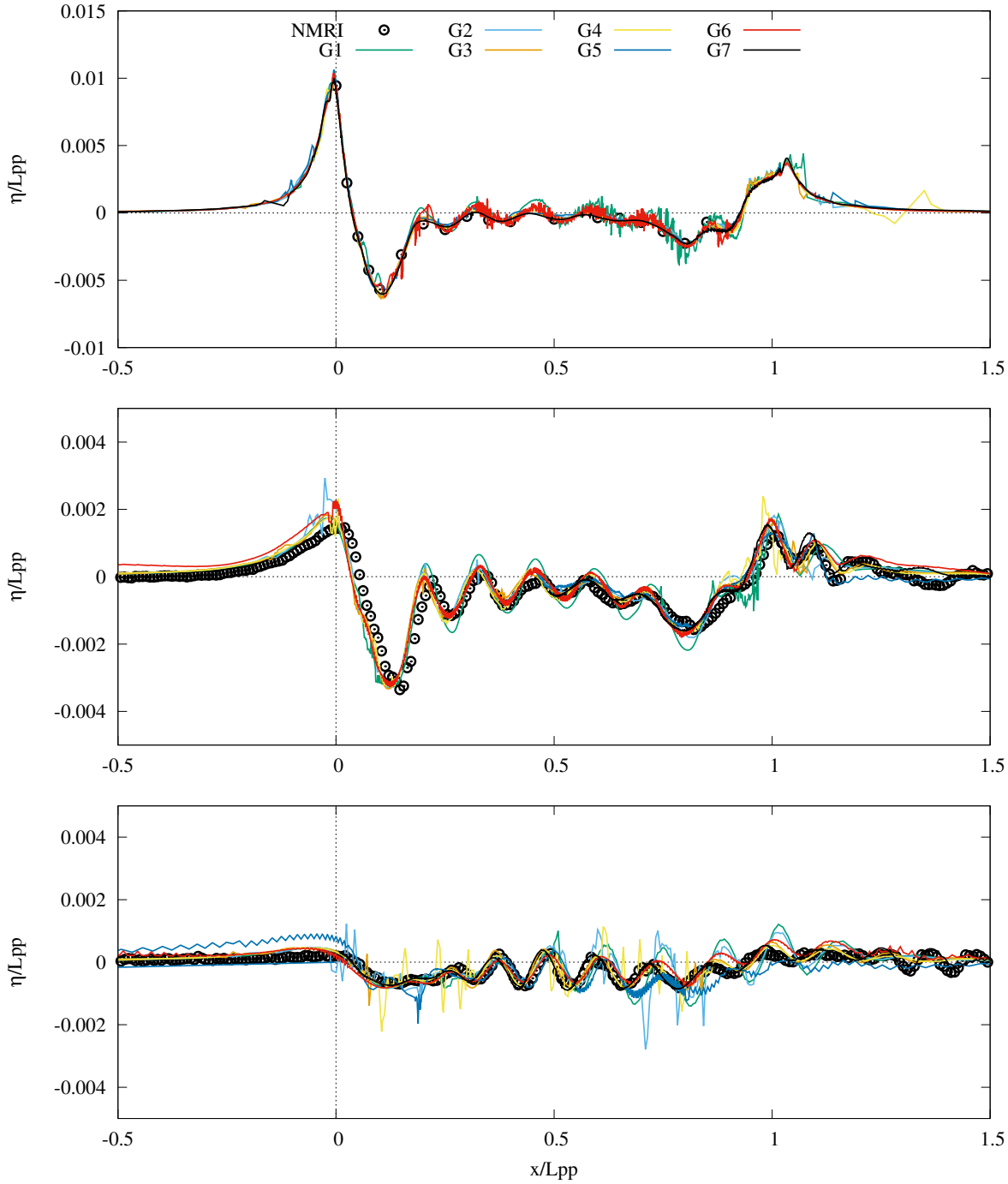

Figure 6: (*top*) profile on hull and $y = 0$, (*middle*) $y/L_{\mathrm{pp}} = 0.1403$ (*bottom*) $y/L_{\mathrm{pp}} = 0.19$.

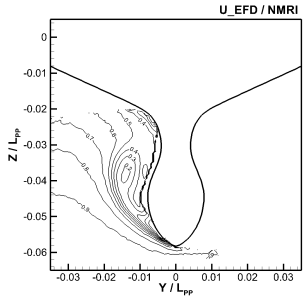

(a) S2:Experiment

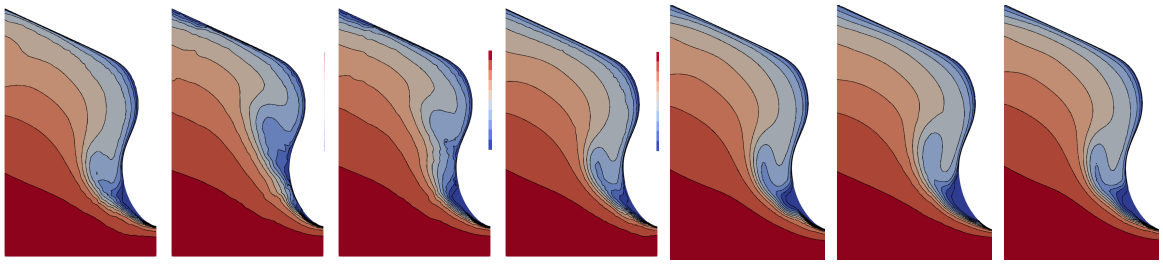

(b) S2: G1-7 from left to right

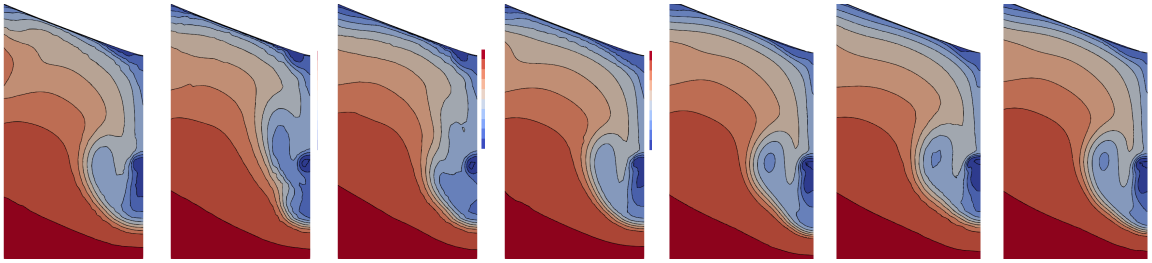

(c) S4, G1-7 from left to right

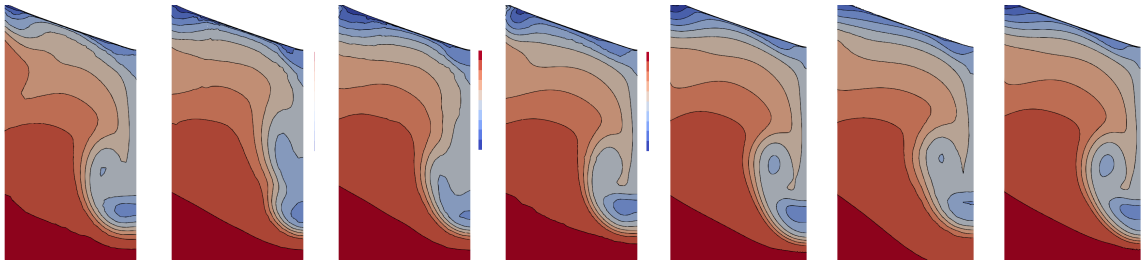

(d) S7, G1-7 from left to right

Figure 7: Comparison of axial velocity in stern planes S2, S4, and S7